Egyptian Journal of Aquatic Biology & Fisheries
Zoology Department, Faculty of Science,
Ain Shams University, Cairo, Egypt.
ISSN 1110 – 6131
Vol. 29(4): 779 – 805 (2025)
www.ejabf.journals.ekb.eg
DOI: 10.21608/EJABF.2025.442279

Decolorization of Methylene Blue Using Chitosan, *Aspergillus caespitosus*, and a Fungal Biomass–Chitosan Composite: Toxicity Assessment using *Daphnia magna*

Ayat Taha[1*], Shaymaa A. Gouda[2] and Amr B. Mostafa[1]
[1]Zoology Department, Faculty of Science, Ain Shams University, Cairo 11566, Egypt
[2]Microbiology Department, Faculty of Science, Ain Shams University, Cairo 11566, Egypt

***Corresponding author: Ayattaha@sci.asu.edu.eg, ayattaha@yahoo.com**

ARTICLE INFO
Article History:
Received: May 30, 2025
Accepted: July 10, 2025
Online: July 16, 2025

Keywords:
Aspergillus caespitosus,
Biosorption,
Chitosan,
Daphnia magna,
Ecotoxicity,
Methylene blue

ABSTRACT

Methylene blue (MB), a cationic dye, is widely utilized in the paper, textiles, pharmaceutical, and ink production industries. The direct discharge of dyes into aquatic environments can cause significant harm to the ecosystem. MB exhibits remarkable stability, rendering its natural decomposition extremely challenging exceedingly difficult. Therefore, it is essential to eradicate the dye and protect the environment from its contamination. This work evaluated the efficacy of removing MB utilizing chitosan, fungal biomass, and a fungal biomass–chitosan composite as biosorbents, along with the subsequent ecotoxicity assessment. The fungal isolate was obtained from water and identified as *Aspergillus caespitosus* (PV449101) using morphological and molecular features. The decolorization process was investigated under optimized conditions, including pH, MB dye concentration, incubation times, and biosorbent dosage. The results indicated that fungal biomass attained 95.58% decolorization of MB at pH 8 within 60 minutes, while chitosan obtained 91.23% at pH 8 and the composite reached 94.18% at pH 10, equilibrating in 120 and 30 minutes, respectively. Fourier transform infrared spectroscopy (FTIR), scanning electron microscopy (SEM), and energy dispersive X-ray (EDX) were employed to assess the biosorbent properties prior to and following the sorption process. This study demonstrated also a considerable reduction in dye zoo-toxicity, as measured by *Daphnia magna*. Acute toxicity was assessed using LC_{50} and calculated toxicity unit (TU) values. Untreated MB was highly toxic. Chitosan reduced toxicity from Class IV to Class III, while fungal biomass achieved Class I status. Notably, the chitosan–biomass composite demonstrated superior detoxification (LC_{50}: 1345 ppm; TU: 0.07), reclassifying MB as slightly toxic. This study presents a novel approach by using *A. caespitosus* and its biomass-chitosan composite for the first time to remove MB from aqueous solutions. Our results proved high decolorization efficiency, combined with eco-friendly and cost-effective properties, and their promising potential in wastewater treatment.

INTRODUCTION

The rapid industrialization of the textile industry has resulted in a substantial rise in wastewater output, presenting serious environmental and human issues due to the durability and resistance of synthetic dyes **(Ali *et al.*, 2022; Taha *et al.*, 2023)**.

Methylene blue (MB), a widely utilized thiazine cationic dye, is often released into aquatic environments, diminishing water clarity, restricting solar penetration, and impairing photosynthetic processes, which results in both acute and chronic toxicity **(Li *et al.*, 2019; Silva *et al.*, 2019; Taha & Gouda, 2025)**.

Traditional physicochemical treatment procedures are expensive, produce harmful byproducts, and are not adaptable to various dye contaminants **(Aksu, 2005; Padmesh *et al.*, 2005)**. Biological decolorization, which encompasses biosorption, biodegradation, and bioaccumulation, has emerged as a sustainable solution to address this issue. Biosorption has attracted significant interest as an effective technique for treating dye-contaminated water utilizing various biosorbents **(Kaushik & Malik, 2009; Silva *et al.*, 2019; Gouda *et al.*, 2023)**.

Chitosan, extracted from chitin, has garnered interest as a biosorbent owing to its biocompatibility, biodegradability, and capacity to engage with organic and inorganic contaminants **(Li *et al.*, 2020; Wang *et al.*, 2022)**. The extraction of chitosan from crustacean shells and its use in wastewater treatment reduces environmental problems while also contributing to solid waste management. However, its limited solubility in acidic conditions necessitates surface modifications to enhance its efficacy **(Kyzas & Bikiaris, 2015; Rahmi *et al.*, 2019)**. Therefore, in our research, microbial decolorization using fungal biomass is utilized, offering an effective approach due to its ready availability, ability to grow well in inexpensive media, and ease of harvesting. Several fungal species employed as dead biomass exhibit superior capabilities in water decolorization through biosorption, owing to their low toxicity and minimal nutritional demands **(Crini, 2006; Contreras *et al.*, 2019)**. Several fungal species, including *Aspergillus fumigatus*, *Fusarium solani*, and *Trametes versicolor*, have demonstrated significant dye removal capabilities through biosorption **(Casas *et al.*, 2014; Kabbout & Taha, 2014; Chen & Ting, 2015a, b)**. Assessing the toxicity of textile wastewater and treatment efficacy is crucial, with *Daphnia magna* serving as a widely accepted bioindicator **(Peltier & Weber, 1985; Villegas-Navarro *et al.*, 1997; Gouda *et al.*, 2024)**. This freshwater organism is highly sensitive to contaminants and is instrumental in establishing water quality criteria and pollutant limits **(ISO, 1982)**.

The current study aimed to manage the waste from crustacean shells and control environmental issues. The first section of this study investigated the effects of various biosorbents (chitosan, *Aspergillus caespitosus* dead biomass, and fungal biomass-chitosan composite) on the decolorization of MB dye at various main variables, such as initial pH, initial dye concentrations, contact time, and biosorbent concentration. In the second section, the ecotoxicity of the treated dye-polluted waters is investigated using *Daphnia magna* for environmental safety. To the best of our knowledge, this study is the first to document the successful elimination of MB dye utilizing *A. caespitosus* and its biomass-chitosan composite.

MATERIALS AND METHODS

Fungal strain and growth conditions

The fungal strain W15 was obtained from polluted water adjacent to factories along the Ismailia Channel in Cairo, Egypt. Water samples were collected randomly and isolated using the dilution method **(Taha *et al.*, 2023)**. In summary, 1mL of contaminated water was added to 9mL of sterile distilled water and serially diluted to $10^{\wedge -7}$. Approximately 0.1mL of dilution was introduced to potato dextrose agar (PDA) plates supplemented with 100mg/ L chloramphenicol to suppress bacterial proliferation. The inoculated plates were incubated at 28±2°C for seven days to facilitate fungal hyphae growth, monitored regularly until the fungus emerged. By regularly inoculating the growing fungus on PDA media, pure culture was produced and thereafter refrigerated at 4°C.

Identification of fungal strain W15

Morphological identification of fungus W15 was performed using the slide culture technique to examine macroscopic and microscopic characteristics **(Raper & Fennell, 1965)**. The D1/D2 regions of the large-subunit (*28S*) *rRNA* gene were amplified using PCR for molecular identification, employing the primers NL-1 (5′-GCA TAT CAA TAA GCG GAG GAA AAG-3′) and NL-4 (5′-GGT CCG TGT TTC AAG ACG G-3′), utilizing fungal DNA extracted through the Zymo-Spin™ IICR Column. Primers were utilized for PCR amplification under the following parameters **(Gouda *et al.*, 2025)**: an initial denaturation phase at 94°C for 3 minutes, followed by 32 amplification cycles at 94°C for 30 seconds, 56°C for 30 seconds, and 72°C for 90 seconds, concluding with a final extension at 72°C for 10 minutes. The amplified products were sequenced with ABI 3730×1 DNA sequencers (GATC, Germany), and a BLAST search was conducted to compare the sequence data with that available at the National Center for Biotechnology Information (NCBI) (https://www.ncbi.nlm.nih.gov/). A phylogenetic analysis was subsequently performed to investigate its relationship with other closely related fungi, employing the neighbor-joining method in MEGA 11 software, with reliability evaluated through 1,000 bootstrap replications **(Tamura *et al.*, 2011)**. The phylogenetic tree was subsequently visualized utilizing the interactive tree of life software (iTOL v.7) (https://itol.embl.de/) **(Letunic & Bork, 2021)**.

Preparation of fungal biomass biosorbent

Mycelial discs from a 5–7-day-old pure *A. caespitosus* fungal culture were inoculated into 100mL of potato dextrose broth (PDB) and incubated at 28±2°C under static conditions with intermittent shaking. Following a seven-day period, the biomass was harvested, rinsed with sterile distilled water, autoclaved at 121.5°C for 15 minutes, subsequently dried, pulverized into a fine powder, and sieved through a 150-mesh screen. The prepared biomass was preserved in a desiccator till further utilization **(Erdem & Cihangir, 2018)**.

Preparation of chitosan polymer biosorbent

Chitosan was extracted from Egyptian shrimp shells following the method of **Kandile *et al.* (2018)**. The shells were thoroughly cleaned, dried at 55°C for 24 hours, and then boiled in 4% NaOH for one hour. After cooling, they were demineralized in 1% HCl for 24 hours and crushed into particles (0.5– 5mm). The material underwent further treatment with 2% NaOH for one hour, followed by boiling in 50% NaOH at 115°C for two hours. The resulting product underwent filtration, and oven-dried at 110°C for six hours and was subsequently stored as chitosan.

Preparation of fungal biomass–chitosan composite

A composite was synthesized with a 1:3 ratio of chitosan to *A. caespitosus* fungal biomass. Chitosan (7.5 g) was solubilized in 100mL of 1% (v/v) acetic acid with continuous agitation at 600 rpm for two hours. The purified dead fungal biomass powder (2.5g) was incrementally incorporated into the chitosan solution while agitating at 400–600 rpm for an additional hour. The resultant suspension was dried at 40°C, removed, rinsed, and freeze-dried (Edwards Buch & Holm RV5) prior to utilization **(El Knidri *et al.*, 2018)**.

Preparation, λmax determination, and calibration of methylene blue dye solutions

Methylene Blue (MB) ($C_{16}H_{18}N_3SCl$), of analytical grade, was acquired from Sigma Aldrich (St. Louis, MO, USA). A stock solution (1000mg/ L) was made by dissolving 1.0g of methylene blue in 1L of distilled water. Working solutions with concentrations between 0.5 and 100mg/ L were subsequently prepared via serial dilution, as necessitated by the experimental requirements. The maximum absorbance wavelength (λmax) of MB was ascertained to be 665nm utilizing a UV–Visible spectrophotometer (Hitachi UV1800). Before analysis, all dye solutions were spun at 250 rpm for 10 minutes to achieve homogeneity and eliminate dispersed particles. The pH of each solution was modified using either 0.1 N HCl or 0.1 N NaOH, as necessary.

A standard curve was established for calibration by graphing absorbance values against MB concentrations throughout the linear range of 0 to 16mg/ L. The molar absorptivity constant (K) was derived from the slope of the linear regression equation obtained. The calibration curve was later utilized to ascertain the residual dye concentrations in biosorption investigations (Fig. 1).

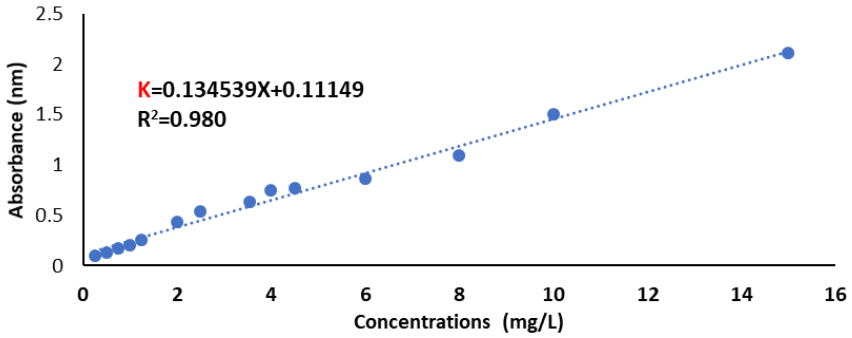

Fig. 1. Calibration curve of methylene blue dye

Decolorization assay using various biosorbents

Batch tests were performed to assess the influence of pH (2–10), dye concentration (5– 80mg/ L), biosorption duration (7.5–120 min), and biosorbent dosage (0.5– 2.5g/ L) on the decolorization of MB. Fifty milliliters of dye solution were transferred to a one-hundred milliliter flask and agitated at 250 revolutions per minute at ambient temperature. The pH was modified utilizing 0.1N HCl or 0.1N NaOH. The absorbance of the filtrate was subsequently quantified using a UV-Vis Spectrophotometer (Hitachi UV1800 UV/VIS) at the specific dye wavelength (665nm) following the filtration of the aqueous layer through Whatman No. 1 filter paper. The optical densities were transformed into concentrations utilizing a pre-established calibration curve, as illustrated in Fig. (1). The percentage of decolorization (%) of various biosorbents calculated using Equation (1) **(Arun & Bhaskara, 2010)**.

$$D = [(\text{Dye (i)} - \text{Dye (f)}) / \text{Dye (i)}] \times 100$$

Where, D represents the decolorization %, dye (i) is the beginning concentration (mg/L), and dye (f) is the final concentration (mg/L). Data are expressed as mean ± standard error from five independent experiments.

Characterization of biosorbents

Fourier transform infrared (FTIR) spectroscopy (Alpha II, Bruker, USA) was employed to identify the functional groups responsible for dye adsorption within the 4000– 400cm^{-1} range. The surface morphology and elemental composition of the biosorbents was analyzed before and after methylene blue adsorption using scanning electron microscopy (SEM) along with energy dispersive X-ray (EDX) (Thermofisher Quanta 250FEG).

Ecotoxicity test

Daphnia magna were purchased from the National Research Center (Cairo, Egypt). The organisms were acclimated for two months in clean media under a 14:10 h light/dark photoperiod and fed *Chlorella* sp. at a rate of 1.6×10^6 cells per individual per day. For acute toxicity assessment, *D. magna* were exposed to varying concentrations of dye-treated water and untreated water under the same photoperiod conditions but without

food. Each concentration group consisted of 10 daphnids, and tests were performed in five replicates. Immobilization and mortality were recorded at 24 and 48 hours. Immobilization was defined as the inability to move within 15 seconds after gentle stimulation, and mortality was confirmed by the absence of cardiac activity, as described by **Taylor *et al*. (2009)**. Acute toxicity units (TUa) were determined using probit analysis, calculated as $TUa = 100/LC_{50}$, where LC_{50} represents the effective concentration causing 50% immobilization **(USEPA, 2002)**. The classification of toxicity was determined according to the European Commission rules (ACE 89/BE 2/D3) presented in Table (1). The experimental design was conducted in the Aquatic Environment Laboratory, Zoology Department, College of Science, Ain Shams University, Cairo, Egypt.

Table 1. The toxicity classification based on TUa values

Class	TUa Range	Toxicity Level
Class I	$TUa < 0.4$	Non-toxic
Class II	$0.4 \leq TUa < 1.0$	Low toxicity
Class III	$1.0 \leq TUa < 10$	Toxic
Class IV	$10 \leq TUa \leq 100$	Highly toxic
Class V	$TUa > 100$	Extremely toxic

Ethical consideration

The Research Ethics Committee of Ain Shams University accepted this work (ASU-SCI/ZOOL/2025/3/4). All efforts were undertaken to reduce the suffering of *Daphnia*, and only a restricted number of organisms were utilized to get scientifically accurate results.

Statistical analysis

Minitab V17 for Windows (Minitab Inc., USA) was used for statistical analysis. Results were provided as mean±standard error of five repeats in all experiments. The data were analyzed using one-way ANOVA and Tukey's multiple comparison test for significant differences ($P< 0.05$).

RESULTS AND DISCUSSION

Identification of fungal isolate

Both macroscopic and microscopic analyses of the isolated fungus W15 in the current study revealed that it belongs to the genus *Aspergillus* and subgenus Nidulantes. Macroscopic evaluation revealed that the isolate W15 appeared as dispersed dark green colonies with a yellow reverse on PDA at 28±2°C. On the other hand, microscopic analysis of the same media revealed the presence of septate hyaline hyphae with thick, smooth walls that developed into pyriform to spathulate vesicles with biseriate metulae covering half to two-thirds of the vesicle, which bore spherical conidia with rough walls (Fig. 2).

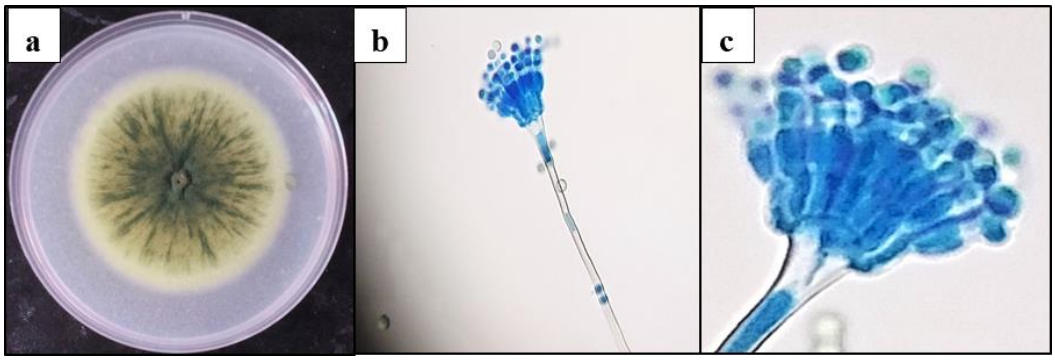

Fig. 2. Morphological characteristics of fungal isolate W15. (a) Colonies cultivated for 7 days on PDA plates at 28±2°C, (b) Conidial heads and conidiophores, and (c) Conidia exhibiting vesicles and metulae

The molecular identification using D1/D2 LSU sequencing was used to confirm the morphological identification due to its adequate length and specificity relative to the *ITS* regions **(Young *et al*., 2022; Ahmed *et al*., 2025)**. The strain W15 exhibited a 100% sequence similarity with *Aspergillus caespitosus* in BLAST sequence alignment analysis. The fungal isolate was identified as *A. caespitosus* through morphological and genetic analysis. The nucleotide sequence was submitted to GenBank and assigned the accession number PV449101. A phylogenetic tree based on neighbor-joining analysis was constructed to compare *A. caespitosus* (PV449101) with the strains of related fungi obtained from NCBI (Fig. 3).

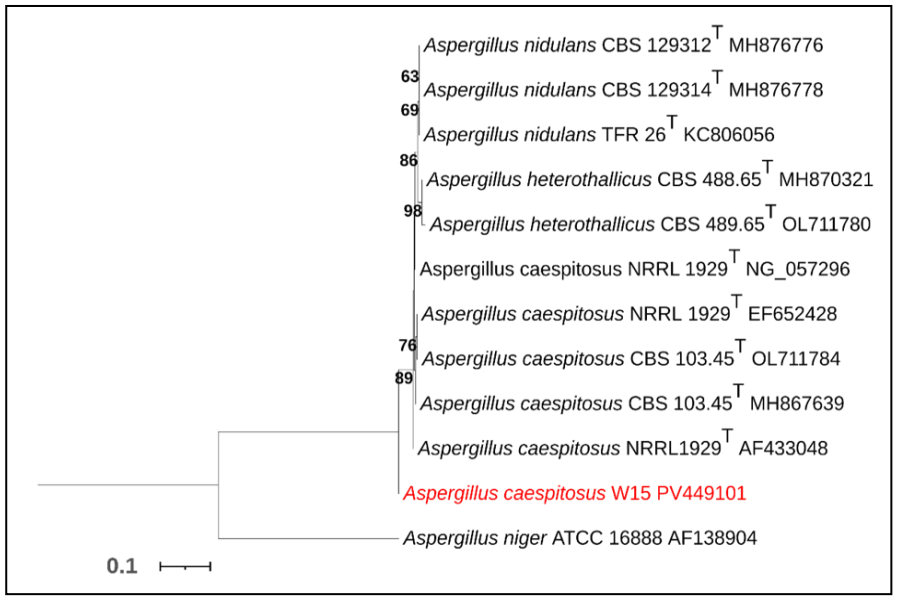

Fig. 3. Phylogenetic relationship between *Aspergillus caespitosus* W15 (PV449101) in red and its related species obtained from NCBI. The filamentous fungus *Aspergillus niger* served as an outgroup. T denotes the type strains of species. Bootstrap values were calculated across 1000 replication.

Numerous *Aspergillus* species are prevalent filamentous fungi commonly located in soil, air, and diverse aquatic environments, such as rivers, distribution systems, and polluted waterways **(Nourmoradi *et al.*, 2012)**. Reports of **Arvanitidou *et al*. (2000)**, **Brandi *et al*. (2007)** and **Sharma and Shaista (2011)** indicated that *Aspergillus* is one of the most frequently isolated species in aquatic environments. *A. caespitosus* was originally detected in the waters of the Bahar Al-Najaf depression **(Al Hatimi & Mutlag, 2022)**. In addition, it was found in enriched wastewater **(Srinivasan *et al.*, 2021)**.

Our research primarily concentrates on the utilization of several biosorbents, including chitosan, *A. caespitosus* biomass, and a fungal biomass-chitosan composite. Biomass has properties of a biologically generated ion exchanger, similar to a chemical molecule **(Saraf & Vaidya, 2015)**. Utilizing shell chitosan as a biosorbent for wastewater treatment contributes to solid waste management and mitigates disposal challenges **(Dhananasekaran *et al.*, 2016)**. Due to the necessity of diverse medium conditions, such as pH, nutrients, and optimal temperature for effective biomass-based biosorption, dead fungal biomass (heat-inactivated via autoclaving) has been employed more frequently than live biomass **(Lan Chi *et al.*, 2023)**. Moreover, the preservation of dead fungal biomass for prolonged durations is straightforward **(Clocchiatti *et al.*, 2020)**. The application of powdered dead fungal biomass increases surface area and inhibits particle aggregation, hence boosting biosorption capability **(Taha *et al.*, 2023b)**. Prior research has shown that *Aspergillus caespitosus* can remove and recover heavy metals (Pb^{+2}) from polluted water sources **(Aftab *et al.*, 2012; Aftab *et al.*, 2017)**. To the best of our knowledge, this is the first report on the biosorption of MB dye by *A. caespitosus*.

Effect of pH on dye decolorization efficiency

The pH of the solution exerted a pronounced influence on the dye removal efficiency of chitosan, biomass, and their composite (Mix), as illustrated in Table (2). All biosorbents displayed minimal adsorption under highly acidic conditions, particularly at pH 2, where excessive protonation likely inhibited the availability of active binding sites through competitive adsorption **(Al-Qudah *et al.*, 2014)**. As the pH increased, dye decolorization efficiency significantly improved substantially across all materials, reaching a maximum at pH 10 for the composite that exhibited the highest significant efficiency (87.89%). Under alkaline conditions (pH 8), biomass and chitosan demonstrated the most significant decoloration percentages of 79.04 and 63.69%, respectively, while chitosan remained less effective. At intermediate pH levels, a nuanced performance profile emerged. Biomass showed relatively better efficacy at pH 4, suggesting greater acid tolerance.

This pattern reflects the ionization dynamics of functional groups—particularly carboxyl and hydroxyl moieties—on the sorbent surfaces. At diminished pH, these groups experience protonation, resulting in electrostatic repulsion and decreased adsorption. Under contrast, deprotonation under alkaline conditions enhances the

electrostatic interactions between negatively charged adsorbent surfaces and cationic dye molecules **(Zhang *et al*., 2015; Chen *et al*., 2018; Gouda & Taha, 2023)**.

Importantly, the chitosan–biomass composite consistently outperformed individual components under alkaline conditions. This synergistic effect likely results from the integration of structurally diverse functional groups and increased porosity, which enhances the availability and accessibility of adsorption sites. Moreover, the competition between H^+/OH^- ions and dye molecules at extreme pH conditions also influenced adsorption capacity, particularly under highly acidic or basic environments, where site competition led to diminished uptake **(Al-Qudah *et al*., 2014)**.

Table 2. Effect of initial pH on decolorization efficiency (%)

pH	Chitosan	Biomass	Fungal Biomass–Chitosan Composite
2	24.74±0.68^{e}	24.84±0.03^{e}	28.79±1.69^{d}
4	30.03 ±1.24^{d}	45.92±0.04^{d}	30.02± 0.25^{d}
6	46.61±0.03^{c}	66.98±0.03^{c}	69.92±0.03^{c}
8	63.69±0.01^{a}	79.046±0.03^{a}	75.99±0.03^{b}
10	59.80±0.013^{b}	78.57±0.03^{b}	87.89±0.03^{a}

Biosorption conditions: Temperature (T)= 28°C; initial dye concentration (Ci)= 20g/L; contact time (t)= 30 minutes; and biosorbent dose (D)= 1g/L. Results are expressed as mean values (n= 5) ± standard error (SE). Different superscript letters within the same column indicate statistically significant differences ($P< 0.05$), according to Tukey's multiple comparison test.

Effect of initial dye concentration on decolorization efficiency

The impact of initial MB concentration (5– 80mg/ L) on dye removal performance is presented in Table (3). At lower concentrations (5mg/ L), biomass demonstrated superior decolorization efficiency of 84.44%, followed by the composite (78.98%) and chitosan (48.53%). These trends are attributable to the higher ratio of available active sites relative to dye molecules at low concentration levels.

However, as dye concentration increased, the performance of the composite significantly improved, surpassing both biomass and chitosan. At 80mg/ L, the composite achieved a significant decolorization efficiency of 89.69%, compared to 63.99% for biomass and only 35.58% for chitosan. The observed decline in chitosan's performance under higher concentrations suggests a saturation of its limited active sites and reduced mass transfer efficiency. Conversely, the superior performance of the composite is attributed to its heterogeneous binding domains, increased surface area, and improved intraparticle diffusion properties, which enhance tolerance to dye saturation and facilitate higher adsorption capacity under elevated pollutant loads.

These results suggest that while biomass is effective at low pollutant concentrations, the composite exhibits enhanced adsorption across a wider concentration range, making it a more robust candidate for high-strength dye effluents.

Table 3. Effect of initial dye concentration on decolorization efficiency (%)

Dye Concentration (g/L)	Chitosan	Biomass	Fungal Biomass–Chitosan Composite
5	48.53±0.30^{c}	84.44±0.086^{b}	78.988±0.109^{e}
10	45.09±0.40^{d}	85.31±0.043^{a}	82.728±0.043^{d}
20	63.81±0.076 ^{b}	79.02±0.021^{c}	87.54±0.32^{b}
40	79.15±0.154^{a}	65.92±0.006^{d}	85.481±0.009^{c}
80	35.58±0.5^{e}	63.99±0.007^{e}	89.697± 0.005^{a}

Biosorption conditions: Temperature (T) = 28°C; pH= 8 for chitosan and biomass, and pH= 10 for the composite; contact time (t)= 30 minutes; and biosorbent dose (D)= 1 g/L. Data are presented as mean values (n= 5) ± standard error (SE). Different superscript letters within the same column indicate statistically significant differences ($P< 0.05$), according to Tukey's multiple comparison test.

Effect of contact time on dye decolorization efficiency

The influence of contact time (7.5–120 min) on dye removal efficiency is shown in Table (4). All biosorbents exhibited rapid initial adsorption, particularly within the first 60 minutes, driven by a high concentration gradient and numerous vacant adsorption sites. Biomass showed the most significant decolorization, achieving 89.1% removal at 60 minutes and maintaining stability at 86.54% after 120 minutes. The composite followed closely, reaching a maximum of 83.09% at 30 minutes with a slight decline to 80.33% at 120 minutes, possibly due to minor desorption or surface saturation effects.

In contrast, chitosan displayed a slower adsorption profile, increasing from 65.65% at 7.5 minutes to 81.56% at 120 minutes. This is likely due to slower internal diffusion and limited accessibility of its adsorption sites. The general trend observed of rapid uptake followed by an equilibrium plateau is consistent with previous studies **(El-Sayed, 2011; Olgun & Atar, 2012; Elaigwu *et al.*, 2014; Garba *et al.*, 2019)**. The initial rapid phase is attributed to abundant vacant binding sites, while the later stage involves gradual dye diffusion into the internal pores of the biosorbents. The data support the use of biomass and the composite for fast-acting dye removal applications, with optimal performance that typically reached within 60 minutes.

Table 4. Effect of time contact on decolorization efficiency (%)

Time of Contact (min.)	Chitosan	Biomass	Fungal Biomass–Chitosan Composite
7.5	65.65±0.037^{e}	75.886±0.0838^{e}	64.97±0.03^{e}
15	73.33±0.013^{d}	79.258±0.0599^{d}	69.02±0.09^{d}
30	79.001±0.014^{c}	85.044±0.0495^{c}	83.09± 0.006^{a}
60	80.292±0.02^{b}	89.34±0.085^{a}	81.78±0.004^{b}
120	81.56±0.108^{a}	86.542±0.0498^{b}	80.33±0.006^{c}

Biosorption conditions: Temperature (T)= 28°C; pH= 8 for chitosan and biomass, and pH= 10 for the composite; biosorbent dose (D)= 1g/L; and initial dye concentrations of 40g/L for chitosan, 10g/L for biomass, and 80g/L for the composite. Data are expressed as mean values (n= 5) ± standard error (SE). Different superscript letters within the same column indicate statistically significant differences ($P< 0.05$), according to Tukey's multiple comparison test.

Effect of biosorbent dosage on dye decolorization efficiency

Biosorbent dosage is a critical parameter affecting adsorption efficiency and operational feasibility. Table (5) illustrates the removal efficiency across different dosages (0.5– 2.5g/ L). At the lowest dose (0.5g/ L), biomass achieved the highest removal (87.52%), followed by chitosan (75.03%) and the composite (47.5%). The lower initial performance of the composite may be attributed to steric hindrance and limited surface area exposure at low concentrations **(Zango *et al*., 2022)**.

As dosage increased, all biosorbents demonstrated significant improvement. At 1.5g/ L, fungal biomass exceeded 90% removal efficiency. At 2.5g/ L, biomass peaked at 95.5%, the composite maintained over 90%, and chitosan reached 88.87%. The increased dosage correlates with greater active site availability, promoting enhanced adsorption. Notably, the composite transitioned from initial underperformance to parity with biomass at higher dosages, indicating its ability to maximize site utilization and support effective dye capture in high-loading treatment scenarios.

Table 5. Effect of biosorbent dosage of chitosan on decolorization efficiency (%)

Biosorbent Concentration (g/L)	Chitosan	Biomass	Fungal Biomass–Chitosan Composite
0.5	75.031±0.05^{d}	87.527±0.0353^{e}	47.50±0.24^{e}
1	80.88±0.39^{c}	89.056±0.0596^{d}	83.10± 0.005^{d}
1.5	87.78±0.004^{b}	93.544±0.0371^{c}	87.74±0.06^{c}
2	91.23±0.8^{a}	93.946±0.0665^{b}	89.712± 0.019^{b}
2.5	88.87±0.004^{b}	95.584±0.0336^{a}	94.18±0.017^{a}

Biosorption parameters: Temperature (T)= 28° C; pH= 8 for chitosan and fungal biomass, and pH= 10 for the biomass–chitosan composite; starting dye concentrations of 40g/L for chitosan, 10g/L for biomass, and 80g/L for the composite. The contact durations were 120 minutes for chitosan, 60 minutes for biomass, and 30 minutes for the composite. Data are expressed as means (n= 5) ± standard error (SE). Distinct superscript letters within the same column denote statistically significant differences (P< 0.05), in accordance with Tukey's multiple comparison test.

Scanning electron microscopy observation and energy dispersive X-ray measurement

Morphological examinations of the utilized biosorbents were performed before and after dye adsorption employing scanning electron microscopy (SEM) and energy dispersive X-ray (EDX), which is regarded as an effective instrument for assessing the elemental and chemical composition of biosorbents **(Dadrasnia *et al*., 2015)**. **Bouras *et al*. (2020)** assert that the presence of surface cavities, along with differences in particle size and morphology, enhances the biosorbent's capacity to adsorb dye molecules.

The SEM micrograph of the chitosan particles showed a network-like structure of the elongated and fibrous character (Fig. 4a). The EDX analysis revealed that the major components of the chitosan polymer are carbon (C), nitrogen (N), and oxygen (O). Minute amounts of calcium (Ca) and iron (Fe) were detected, perhaps from the natural origin or residues from the processing process (Fig. 4c). The fibrous structure of chitosan and its network-like, connected structures are filled with methylene blue dye (MB) after biosorption, and the EDX spectrum undergoes significant change: the emergence of sulfur (S) on the chitosan surface. As MB contains sulfur ($C_{16}H_{18}ClN_3S$), the emergence of this element in the post-treatment spectrum is the direct evidence that MB molecules were effectively adsorbed on the chitosan surface (Fig. 4b, d). This finding concurs with other adsorption studies in which detection by sulfur confirmed adsorption of the dye **(Sabar *et al*., 2020; Hidayat *et al*., 2022; Saeed *et al*., 2022)**.

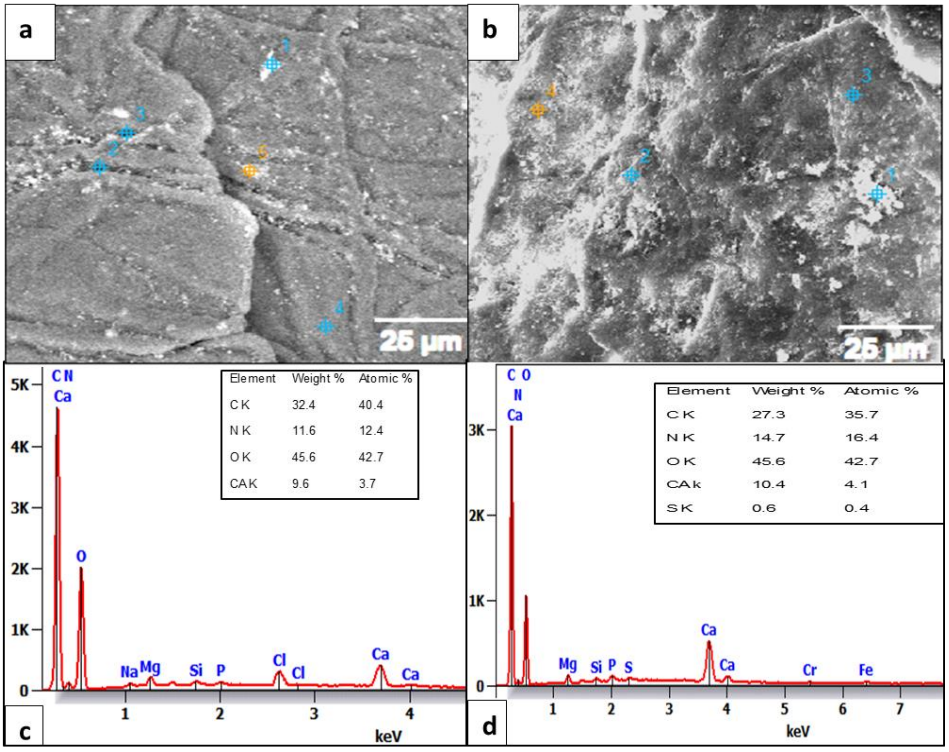

Fig. 4. Scanning electron microscopy (SEM) coupled with energy dispersive X-ray (EDX) analysis of chitosan: (a, b) SEM images of chitosan prior to and subsequent to methylene blue (MB) adsorption, respectively; (c, d) EDX spectra of chitosan before and after MB adsorption, respectively

In contrast, prior to dye adsorption, the heat-treated biomass of *A. caespitosus* displayed an aggregate rough and porous surface of filamentous particles with uneven and broken edges (Fig. 5a). The EDX spectra showed that carbon and oxygen predominated, reflecting its organic nature. Since they are mineral components found in the cytoplasm and cell wall of fungi, additional components such as magnesium (Mg), silicon (Si), phosphorus (P), sulfur (S), potassium (K), calcium (Ca), and iron (Fe) were included as illustrated in Fig. (5c). The MB dye clearly affected the surface morphology of the biomass. Following MB treatment, the initial overall surface porosity and roughness decreased by the adsorbed because the dye molecules were trapped in the particle pores, concealing the bordered relief that defined the surface of the dead biomass of *A. caespitosus* (Fig. 5b). This finding agrees with the elemental pattern, which was qualitatively identical, but one major difference was observed: an increased intensity of peaks of sulfur as depicted in Fig. (5d). This increase is attributed to the adsorption of sulfur-bound MB dye onto biomass. Although the original natural fungal material possessed some sulfur content, comparative improvement after treatment vastly favors the successful incorporation of the dye. Minor variations in the amount of the other elements, e.g., increased iron and decreased potassium and chlorine, were also noted, which can indicate surface interaction or ion exchange upon adsorption, as observed with

the example of fungal-based adsorbent studies **(Ozudogru & Tekne, 2023; Sylvia *et al.*, 2023; Gollakota, 2025)**.

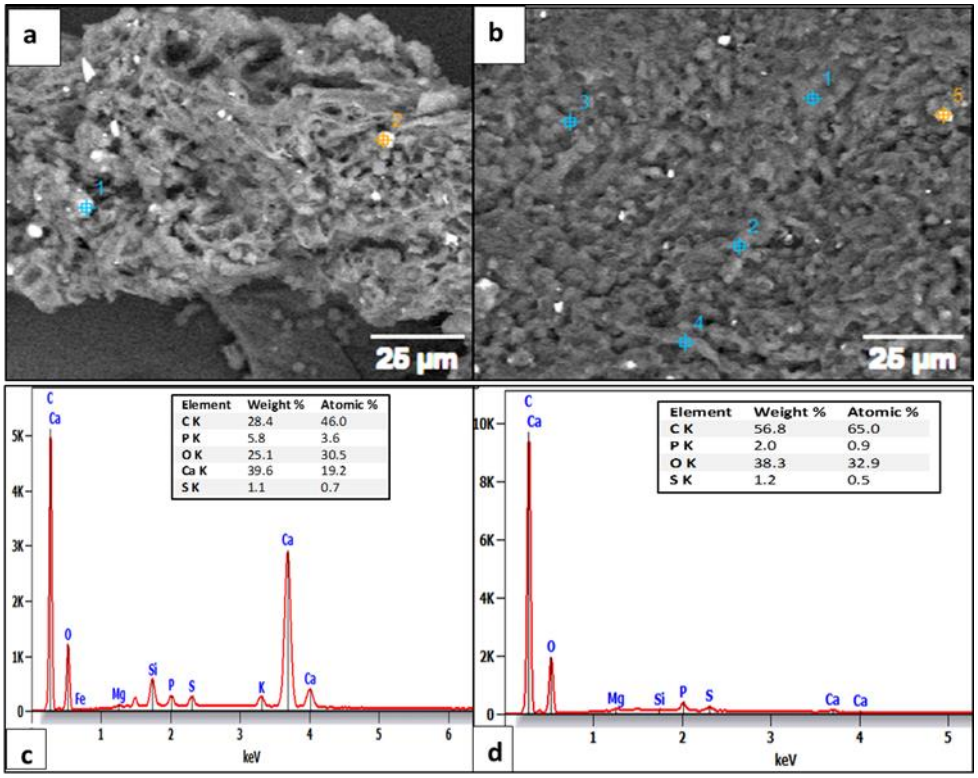

Fig. 5. Scanning electron microscopy (SEM) coupled with energy dispersive X-ray (EDX) analysis of fungal biomass (*A. caespitosus*): (a, b) SEM micrographs of fungal biomass prior to and subsequent to MB adsorption, respectively; (c, d) EDX spectra of fungal biomass before and after MB adsorption, respectively

On the other hand, as shown in Fig. (6a, b), the fungal biomass–chitosan composite surface exhibits more obvious pores or cracks than chitosan, which improved MB adsorption. Prior to adsorption, EDX analyses showed a combination of elemental peaks, corresponding to both materials (Fig. 6c). Some of the dominant elements were C, N, and O (from chitosan), along with mineral elements Na, Al, Si, P, Cl, K, and Ca that are typical for fungal biomass. Sulfur was either absent or below the limit of detection. After MB adsorption, sulfur was certainly present in different regions of the composite and showed a considerable increase compared to the untreated material. Enrichment of sulfur is excellent evidence that MB was successfully adsorbed onto the composite material. The post-treatment profile also showed some alteration in mineral composition, notably the reduction of potassium and chlorine and the appearance of iron in some regions (Fig. 6d). These results are in line with the fact that the composite material not only shows the sum of the adsorption activity of the components but also exhibits greater dye capture efficiency, as indicated by greater sulfur content. Similar results have been

reported before in studies involving biopolymer-mineral composites for adsorbing dyes **(Hidayat *et al*., 2022; Gollakota, 2025)**.

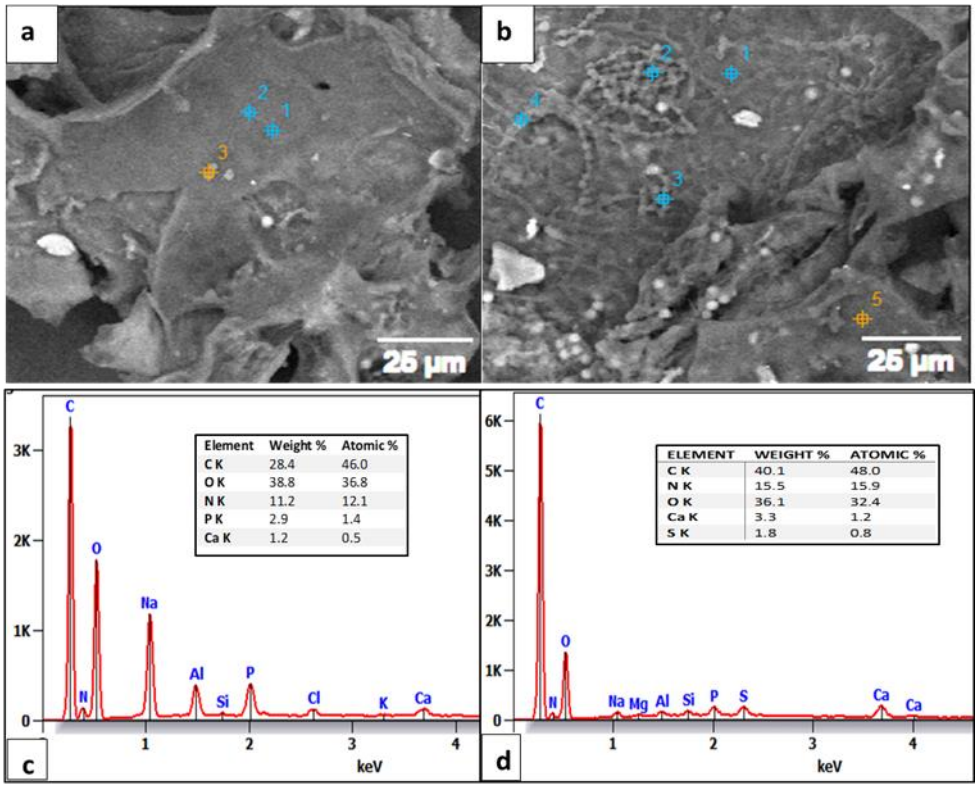

Fig. 6. Scanning electron microscopy (SEM) combined with energy dispersive X-ray (EDX) analysis of a fungal biomass–chitosan composite: (a, b) SEM images of the composite prior to and following MB adsorption, respectively; (c, d) EDX spectra of the composite prior to and following MB adsorption, respectively

The aforementioned findings demonstrated the fungal biomass's strong attraction for cationic dye, which is thought to be the most efficient method of removing MB dye from wastewater.

Fourier-transform infrared (FTIR) spectroscopic analysis of adsorbent materials

Fourier-Transform Infrared (FTIR) spectroscopy revealed the functional group dynamics and adsorption behavior of three adsorbent materials (chitosan, fungal biomass, and its composite) before and after interaction with methylene blue (MB) dye. The spectral shifts and intensity changes across all materials showed strong evidence of functional group involvement in MB binding, which occurred mainly through hydrogen bonding, electrostatic interactions, and limited physisorption.

Chitosan, a biopolymer rich in amine and hydroxyl functional groups, had peaks at 3355 cm^{-1} (O–H/N–H stretching), 2920 cm^{-1} (C–H), 1636 cm^{-1} (amide I), and 1418

cm^{-1} (N–H bending) before dye exposure, consistent with polysaccharide and glucosamine units **(Osman & Arof, 2003)**. Upon MB adsorption, there were significant changes: the broad band was shifted to 3273 cm^{-1}, amide I to 1582 cm^{-1} and aliphatic –CH to 2872 cm^{-1}. The changes, especially on the hydroxyl and amine bands, confirm the active role of these groups in dye immobilization, although the absence of new MB specific peaks confirms physisorption was the dominant mechanism (Fig. 7a) (**Szadkowski & Marzec, 2024)**.

Fungal biomass is a more complex matrix of proteins, lipids, polysaccharides, and several functional groups **(Crini, 2006)**. Pre-treatment spectra of *A. caespitosus* had a broad –OH/–NH stretch at 3279 cm^{-1} and peaks for –CH, C=O and C–N functionalities. After MB interaction, only minor shifts were observed (e.g. 3279 to 3272 cm^{-1}, 1632 to 1629 cm^{-1}) which were indicative of weak physical interactions rather than chemical bonding (Fig.7b). The slight displacements corroborate previous findings that the active groups on the fungal cell surface engage with the aromatic rings of dye molecules via weak physical forces such as Van der Waals and hydrogen bonds, in addition to chemical and electrostatic interactions **(Marcharchand & Ting, 2017; Salvi *et al*., 2017; Smith, 2022)**. Comparable functional groups were identified in the investigations conducted by **Yang *et al*. (2011)**, **Chaudhry *et al*. (2014)** and **Chen *et al*. (2019)**, which utilized autoclaving of dead fungal cells in the dye biosorption process.

In contrast, the fungal biomass-chitosan composite (mix) showed synergistic behavior. The composite spectrum was a combination of the two parents but with more intense amide I (1637 cm^{-1}) and additional ones like amide II/ethylenic bond 1548 cm^{-1} **(Huq *et al*., 2022)**. After MB adsorption, significant spectral changes were observed: the emergence of a new aromatic–CH band at 2854 cm^{-1} and a carbonyl band at 1745 cm^{-1} clearly showed MB immobilization. Notably, the 1548 cm^{-1} band shifted to 1596 cm^{-1} which is consistent with interaction with the aromatic and amide groups of MB (Fig. 7c). These extensive changes, including a decrease in –OH, –NH, and C–N intensity, indicate a more complex and stronger adsorptive mechanism than the constituent materials, and the composite takes advantage of both chemical and physical interactions for better dye removal **(Ovchinnikov *et al*., 2016)**.

In total, FTIR analysis revealed a hierarchy of functional group activity and strength of interaction: physisorption was favored by fungal biomass (*A. caespitosus*), more targeted functional group interactions were engaged with chitosan, and the composite exhibited synergistic adsorption with evidence of new bond formation and enhanced interaction with MB dye than chitosan. This is encouraging for the potential of composite biomaterials for efficient wastewater dye remediation.

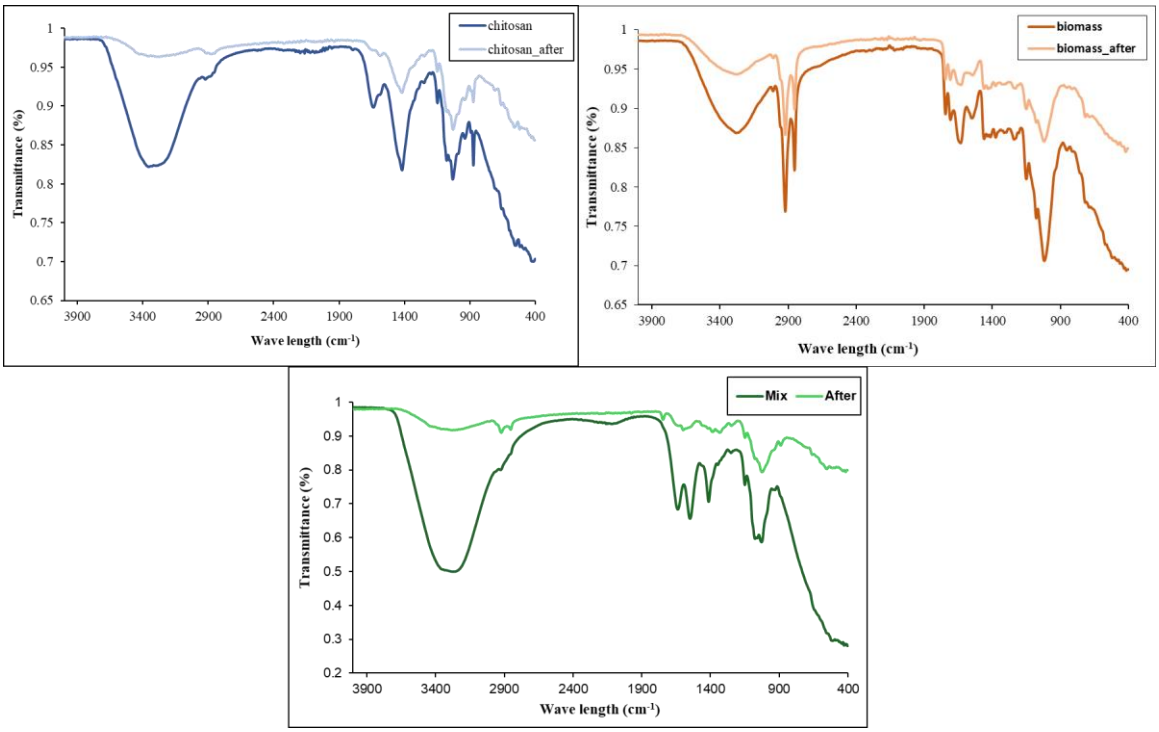

Fig. 7. FTIR spectrum of biosorbents before and after MB adsorption*:* (a) Chitosan before and after MB adsorption; (b) Fungal biomass before and after MB adsorption, and (c) Fungal biomass–chitosan composite (Mix) before and after MB adsorption

Toxicity classification based on LC_{50} and toxicity units (TU)

Ecotoxicological assessment is a crucial step in evaluating the environmental impact of treated wastewater, particularly regarding residual toxicity toward aquatic organisms. Among various bioindicators, *Daphnia magna* is widely recognized for its sensitivity and reliability in acute toxicity testing and has been extensively employed in previous studies **(Elisangela *et al.*, 2009; Porri *et al.*, 2011)**. It has been reported that fungal and biological treatment processes can lead to a measurable reduction in the toxicity of dye-laden effluents **(Casieri *et al.*, 2008; Przystaś *et al.*, 2015)**.

In the present study, the zootoxicity of methylene blue (MB) before and after treatment with chitosan, *A. caespitosus* fungal biomass, and the fungal biomass–chitosan composite was evaluated using *D. magna*, with corresponding LC_{50} values and toxicity units (TU) calculated to quantify ecological risk (Table 6). The untreated MB solution exhibited severe acute toxicity, with LC_{50} values of 7 ppm at 24 hours and 1.8 ppm at 48 hours. These values classify it within Toxicity Class IV (Highly Toxic), corresponding to TU values of 14.3 and 55.6 at 24 and 48 hours, respectively.

Following treatment, notable reductions in toxicity were observed across all biosorbents. Chitosan-treated effluent showed a moderate improvement in safety, as evidenced by increased LC_{50} values of 19 ppm (TU = 6.7) at 24 hours and 20.6 ppm (TU = 4.9) at 48 hours. This repositioned the effluent into toxicity Class III (Toxic), indicating partial detoxification. More substantial improvements were achieved with biomass and the composite biosorbent. Biomass treatment resulted in LC_{50} values of 25 ppm (Class III) at 24 hours and a marked increase to 275 ppm (TU = 0.36) at 48 hours, categorizing the effluent as toxicity Class I (Non-toxic) after extended contact. The most pronounced detoxification was observed with the chitosan–biomass composite, which elevated the LC_{50} from an initial 17.8 ppm at 24 hours (Class III) to an exceptional 1345 ppm at 48 hours, reducing TU to 0.07 and firmly placing the treated water in toxicity Class I (Non-toxic).

These findings clearly demonstrate the enhanced ecotoxicological safety of treated dye solutions, particularly when using the composite biosorbent. The fungal biomass–chitosan composite appears to leverage the individual strengths of both materials—chitosan's chemical functionality and biomass's high surface activity to achieve synergistic effects than chitosan that lead to highly effective detoxification. The steep decline in toxicity units (TU < 0.1) following composite treatment underscores its potential as a sustainable, eco-friendly solution for wastewater purification, suitable for safe discharge into natural water bodies without posing significant harm to aquatic ecosystems.

Table 6. Toxicity evaluation of untreated and treated MB dye using *D. magna*

Treatment	Time (Hr)	LC_{50} (ppm)	TU	Class	Toxicity
Untreated water	24	7	14.3	IV	High
	48	1.8	55.6	IV	High
Chitosan treated water	24	19	6.7	III	Toxic
	48	20.6	4.9	III	Toxic
Biomass treated water	24	25	4	III	Toxic
	48	275	0.36	I	Nontoxic
Composite treated water	24	17.8	5.6	III	Toxic
	48	1345	0.07	I	Nontoxic

CONCLUSION

This study involved the preparation and application of various natural biosorbents to decolorize methylene blue (MB). Under the experimental circumstances employed, the dead fungal biomass exhibited the highest methylene blue removal among the examined biosorbents, achieving a decolorization percentage of 95.58%, followed by composite at 94.18% and chitosan at 91.23%, respectively. The decolorization efficiency of several

biosorbents was influenced by pH, initial dye concentrations, contact duration, and biosorbent dosage. The primary hydroxyl, amino, phosphoryl, alkane, and other functional groups on the surface of fungal biomass are chiefly accountable for the enhanced decolorization of MB dye using this material. In the zootoxicity experiments, the fungal biomass and composite-treated water exhibited significant reductions, declining from class IV (toxic) to III and I (nontoxic) at 24 and 48 hours, respectively, while chitosan-treated water decreased to class III at both 24 and 48 hours, as per the experimental modifications. This study is the first report on the efficacy of the fungus *A. caespitosus* and a fungal biomass-chitosan composite in decolorizing MB dye. This study shown that *A. caespitosus* and its composite had promising applications as environmentally sustainable and cost-effective biosorbents for addressing solid waste disposal challenges and for the decolorization and detoxification of MB dye from aqueous solutions.

AUTHOR CONTRIBUTION

All authors equally contributed to the conception and design of the study, execution of the experiments, data analysis and interpretation, provision of materials, and manuscript writing. All authors have read and approved the final version of the manuscript.

DISCLOSURE STATEMENT

No potential conflict of interest was reported by the author(s).

REFERENCES

Aftab, K.; Akhtar, K. and Jabbar, A. (2012). Process optimization and mechanistic studies of lead (II): *Aspergillus caespitosus* interaction for industrial effluent treatment. Afr. J. Biotechnol., 11(95): 16142–16157. https://doi.org/10.5897/ajb11.4051

Aftab, K.; Akhtar, K. and Noreen, R. (2017). Comparative efficacy of locally isolated fungal strains for Pb(II) removal and recovery from water. Chem. Cent. J., 11: 133. https://doi.org/10.1186/s13065-017-0363-4

Ahmed, M.G.; Gouda, S.A. and Donia, S. (2025). Production of single cell protein by fungi from different food wastes. Biomass Convers. Biorefin., 15: 5447–5462. https://doi.org/10.1007/s13399-024-05478-5

Aksu, Z. **(2005).** Application of biosorption for the removal of organic pollutants: a review. Proc. Biochem., 40: 997–1026.

Al Hatimi, I.A.R. and Mutlag, N.H. (2022). Isolation and identification of fungi from soil and water in the Bahr Al-Najaf Depression. J. Pharm. Negat. Results, 13: 173-191. https://doi.org/10.47750/pnr.2022.13.s02.38

Ali, S.S.; Al-Tohamy, R. and Sun, J. (2022). Performance of *Meyerozyma caribbica* as a novel manganese peroxidase-producing yeast inhabiting wood-feeding termite gut symbionts for azo dye decolorization and detoxification. Sci. Total Environ., 806: 150665. https://doi.org/10.1016/j.scitotenv.2021.150665

Al-Qudah, Y.H.F.; Mahmoud, G.A. and Abdel Khalek, M.A. (2014). Radiation crosslinked poly(vinyl alcohol)/acrylic acid copolymer for removal of heavy metal ions from aqueous solutions. J. Radiat. Res. Appl. Sci., 7(2): 135–145.

Arun, P.A.S. and Bhaskara, R.K.V. **(2010).** Physico-chemical characterization of textile effluent and screening for dye decolorizing bacteria. Glob. J. Biotechnol. Biochem., 5: 80-86.

Arvanitidou, M.; Spaia, S. and Velegraki, A. (2000). High level of recovery of fungi from water and dialysate in hemodialysis units. J. Hosp. Infect., 45: 225–230.

Bouras, H.D.; Isik, Z. and Arikan, E.B. (2020). Biosorption characteristics of methylene blue dye by two fungal biomasses. Int. J. Environ. Stud., 78(3): 365–381.https://doi.org/10.1080/00207233.2020.1745573

Brandi, G.; Sisti, M. and Paparini, A. (2007). Swimming pools and fungi: An environmental epidemiology survey in Italian indoor swimming facilities. Int. J. Environ. Health Res., 17(3): 197–206.

Casas, N.; Parella, T. and Vincent, T. (2014). Metabolites from the biodegradation of triphenyl methane dyes by *Trametes versicolor* or laccase. Chemosphere, 75: 1344–1349. https://doi.org/10.1016/j.chemosphere.2009.02.029

Casieri, L.; Varese, G.C.; Anastasi, A. and Marchisio, V.F. **(2008).** Decolorization and detoxication of reactive industrial dyes by immobilized fungi *Trametes pubescens* and *Pleurotus ostreatus*. Folia Microbiol., 53(1): 44–52.

Chaudhry, M.T.; Zohaib, M. and Rauf, N. (2014). Biosorption characteristics of *Aspergillus fumigatus* for the decolorization of triphenylmethane dye acid

violet 49. Appl. Microbiol. Biotechnol., 98(7): 3133–3141. https://doi.org/10.1007/s00253-013-5306-y

Chen, L.; Wu, P. and Chen, M. (2018). Preparation and characterization of the eco-friendly chitosan/vermiculite biocomposite with excellent removal capacity for cadmium and lead. *Appl.* Clay Sci., 159: 74–82. https://doi.org/10.1016/j.clay.2018.04.005

Chen, S.H. and Ting, A.S.Y. (2015a). Biodecolorization and biodegradation potential of recalcitrant triphenyl methane dyes by *Coriolopsis* sp. isolated from compost. J. Environ. Manag., 150: 274–280. https://doi.org/10.1016/j.jenvman.2014.09.014

Chen, S.H. and Ting, A.S.Y. (2015b). Biosorption and biodegradation potential of triphenylmethane dyes by newly discovered *Penicillium simplicissimum* isolated from indoor wastewater sample. Int. Biodeterior. Biodegrad., 103: 1–7. https://doi.org/10.1016/j.ibiod.2015.04.004

Chen, S.H.; Cheow, Y.L. and Ng, S.L. (2019). Removal of triphenylmethane dyes in single-dye and dye-metal mixtures by live and dead cells of metal-tolerant *Penicillium simplicissimum*. Sep. Sci. Technol., 55(13): 2410–2420. https://doi.org/10.1080/01496395.2019.1626422

Clocchiatti, A.; Hannula, S. E. and van den Berg, M. (2020). The hidden potential of saprotrophic fungi in arable soil: Patterns of short-term stimulation by organic amendments. Appl. Soil Ecol., 147: 103434. https://doi.org/10.1016/j.apsoil.2019.103434

Contreras, M.; Grande-Tovar, C.D. and Vallejo, W. (2019). Bioremoval of methylene blue from aqueous solution by *Galactomyces geotrichum* KL20A. Water, 11(2): 282. https://doi.org/10.3390/w11020282

Crini, G. (2006). Non-conventional low-cost adsorbents for dye removal: A review. Bioresour. Technol., 97: 1061–1085.

Dadrasnia, A.; Wei, K. C. and Shahsavari, N. (2015). Biosorption potential of *Bacillus salmalaya* strain 139SI for removal of Cr (VI) from aqueous solution. Int. J. Environ. Res. Public Health, 12(12): 15321–15338. https://doi.org/10.3390/ijerph121214985

Dhananasekaran, S. and Palanivel, R. (2016). Adsorption of methylene blue, bromophenol blue, and Coomassie brilliant blue by α-chitin nanoparticles. J. Adv. Res., 7(1): 113–124.

El Knidri, H.; Belaabed, R. and Addaou, A. (2018). Extraction, chemical modification and characterization of chitin and chitosan. Int. J. Biol. Macromol., 120: 1181–1189.

Elaigwu, S. E.; Rocher, V. and Kyriakou, G. (2014). Removal of Pb^{2+} and Cd^{2+} from aqueous solution using chars from pyrolysis and microwave-assisted hydrothermal carbonization of *Prosopis africana* shell. J. Ind. Eng. Chem., 20(5): 3467–3473. https://doi.org/10.1016/j.jiec.2013.12.016

Elisangela, F.; Rea, Z. and Fabio, D. G. (2009). Biodegradation of textile azo dyes by a facultative *Staphylococcus arlettae* strain VN-11 using a sequential microaerophilic/aerobic process. Int. Biodeterior. Biodegrad., 63: 280–288. https://doi.org/10.1016/j.ibiod.2008.09.005

El-Sayed, G.O. (2011). Removal of methylene blue and crystal violet from aqueous solutions by palm kernel fiber. Desalination, 272: 225–232. https://doi.org/10.1016/j.desal.2011.01.019

Erdem, Ö. and Cihangir, N. (2018). Color removal of some textile dyes from aqueous solutions using *Trametes versicolor*. Hacet. J. Biol. Chem., 45(4): 499–507.

Garba, Z.N.; Tanimu, A. and Zango, Z.U. (2019). *Borassus aethiopum* shell-based activated carbon as efficient adsorbent for carbofuran. Bull. Chem. Soc. Ethiop., 33(3): 425–436. https://doi.org/10.4314/bcse.v33i3.7

Gollakota, A.R.K.; Subbaiah, M.V. and Singh, A. (2025). Adsorption of methylene blue from aqueous solution using chitosan polymer-impregnated *Tricholoma matsutake* fungal biomass. J. Mol. Liq., 426: 127305.

Gouda, S.A. and Taha, A. (2023). Biosorption of heavy metals as a new alternative method for wastewater treatment: A review. *Egypt.* J. Aquat. Biol. Fish., 27(2): 135–153. https://doi.org/10.21608/ejabf.2023.291671

Gouda, S.A.; Eid, D.M. and Elsharkawy, T.M.F. (2023). Biosorption of cadmium from polluted waters using dead biomass of the fungus *Alternaria tenuissima* and its toxicological effects on male albino rats. *Egypt.* J. Aquat. Biol. Fish., 27(6): 23–58. https://doi.org/10.21608/ejabf.2023.325679

Gouda, S.A.; Hassanein, N.M. and Salah, M. (2025). Antifungal activity of boron/selenium nanoparticles irradiated via gamma rays against *Alternaria alternata* and *Fusarium equiseti*. Curr. Microbiol., 82(3): 129.https://doi.org/10.1007/s00284-025-04089-1

Gouda, S. A.; Hesham, H. and Taha, A. (2024). Bioindicators: A promising tool for detecting and evaluating water pollution. *Egypt.* J. Aquat. Biol. Fish., 28(4): 1209–1235. https://doi.org/10.21608/ejabf.2024.374025

Hidayat, E.; Yonemura, S.; Mitoma, Y. and Harada, H. (2022). Methylene blue removal by chitosan cross-linked zeolite from aqueous solution and other ion effects: Isotherm, kinetic, and desorption studies. Adsorpt. Sci. Technol., (2022): 1–10. https://doi.org/10.1155/2022/1853758

Huq, T.; Khan, A. and Brown, D. (2022). Sources, production and commercial applications of fungal chitosan: A review. J. Bioresour. Bioprod., 7(2): 85–98.

ISO (1982). Water quality—Determination of the inhibition of the mobility of *Daphnia magna* Straus (Cladocera, Crustacea). *ISO 6341:1982*. Geneva, Switzerland: International Organization for Standardization.

Kabbout, R. and Taha, S. (2014). Biodecolorization of textile dye effluent by biosorption on fungal biomass materials. Phys. Procedia, 55: 437–444. https://doi.org/10.1016/j.phpro.2014.07.063

Kandile, N.G.; Zaky, H.T. and Mohamed, M.I. (2018). Extraction and characterization of chitosan from shrimp shells. Open J. Org. Polym. Mater., 8(3): 33–42.

Kaushik, P. and Malik, A. (2009). Fungal dye decolourization: Recent advances and future potential. Environ. Int., 35(1): 127–141. https://doi.org/10.1016/j.envint.2008.05.010

Kyzas, G. Z. and Bikiaris, D. N. (2015). Recent modifications of chitosan for adsorption applications: A critical and systematic review. Mar. Drugs, 13: 312–337. https://doi.org/10.3390/md13010312

Lan Chi, N.T.; Hương, Đ.T.T. and Đạo, P.T. (2023). Biosorption potential of viable and dead *Aspergillus flavus* biomass on polluted pond water. Environ. Res., 232: 116293. https://doi.org/10.1016/j.envres.2023.116293

Letunic, I. and Bork, P. (2021). Interactive Tree of Life (iTOL) v5: an online tool for phylogenetic tree display and annotation. Nucleic Acids Res., 49(W1): W293–W296. https://doi.org/10.1093/nar/gkab301

Li, B. and Elango, J. (2020). Recent advancement of molecular structure and biomaterial function of chitosan from marine organisms for pharmaceutical and nutraceutical application. Appl. Sci., 10(14): 4719. https://doi.org/10.3390/app10144719

Li, J.F.; Rupa, E.J. and Hurh, J. (2019). *Cordyceps militaris* fungus-mediated zinc oxide nanoparticles for the photocatalytic degradation of methylene blue dye. Optik, 183: 691–697. https://doi.org/10.1016/j.ijleo.2019.02.081

Marcharchand, S. and Ting, A.S.Y. (2017). *Trichoderma asperellum* cultured in reduced concentrations of synthetic medium retained dye decolourization efficacy. J. Environ. Manage., 203: 542–549. https://doi.org/10.1016/j.jenvman.2017.06.068

Nourmoradi, H.; Nikaeen, M. and Stensvold, C.R. (2012). Ultraviolet irradiation: An effective inactivation method of *Aspergillus* spp. in water for the control of waterborne nosocomial aspergillosis. Water Res., 46(18): 5935–5940. https://doi.org/10.1016/j.watres.2012.08.015

Olgun, A. and Atar, N. (2012). Equilibrium, thermodynamic and kinetic studies for the adsorption of lead (II) and nickel (II) onto clay mixture containing boron impurity. J. Ind. Eng. Chem., 18(5): 1751–1757. https://doi.org/10.1016/j.jiec.2012.02.038

Osman, Z. and Arof, A.K. (2003). FTIR studies of chitosan acetate-based polymer electrolytes. Electrochim. Acta, 48(8): 993–999. https://doi.org/10.1016/S0013-4686(02)00848-5

Ovchinnikov, O.V.; Evtukhova, A.V. and Kondratenko, T.S. (2016). Manifestation of intermolecular interactions in FTIR spectra of methylene blue molecules. Vib. Spectrosc., 86: 181–189. https://doi.org/10.1016/j.vibspec.2016.07.005

Ozudogru, Y. and Tekne, E. (2023). Adsorption of methylene blue from aqueous solution using spent coffee/chitosan composite. J. Water Chem. Technol., 45(3): 234–245. https://doi.org/10.3103/S1063455X23030085

Padmesh, T.V.N.; Vijayaraghavan, K. and Sekaran, G. (2005). Batch and column studies on biosorption of acid dyes on fresh water macro alga. J. Hazard. Mater., 125(1–3): 121–129. https://doi.org/10.1016/j.jhazmat.2005.05.020

Peltier, W. and Weber, C.I. (1985). Methods for measuring the acute toxicity of effluents to freshwater and marine organisms (EPA/600/4-85/013). U.S. Environ. Prot. Agency, Cincinnati, OH.

Porri, A.; Baroncelli, R. and Guglielminetti, L. (2011). *Fusarium oxysporum* degradation and detoxification of a new textile glycoconjugate azo dye (GAD). Fungal Biol., 115(1): 30–37. https://doi.org/10.1016/j.funbio.2010.10.006

Przystaś, W.; Zabłocka-Godlewska, E. and Grabińska-Sota, E. (2015). Efficacy of fungal decolorization of a mixture of dyes belonging to different classes. Braz. J. Microbiol., 46(2): 415–424. https://doi.org/10.1590/S1517-838246220131246

Rahmi, Fathurrahmi, Lelifajri, Purnamawati, F. and Sembiring, R. (2019). Preparation of magnetic chitosan beads for heavy metal ions removal from water. IOP Conf. Ser. Earth Environ. Sci., 276: 012004. https://doi.org/10.1088/1755-1315/276/1/012004

Raper, K.B. and Fennell, D.I. (1965). *The genus Aspergillus.* Baltimore: Williams & Wilkins.

Sabar, S.; Aziz, H.A. and Yusof, N.H. (2020). Preparation of sulfonated chitosan for enhanced adsorption of methylene blue from aqueous solution. React. Funct. Polym., 151: 104584. https://doi.org/10.1016/j.reactfunctpolym.2020.104584

Saeed, T.; Naeem, A. and Din, I.U. (2022). Synthesis of chitosan composite of metal-organic framework for the adsorption of dyes: Kinetic and thermodynamic approach. J. Hazard. Mater., 427: 127902. https://doi.org/10.1016/j.jhazmat.2021.127902

Saraf, S. and Vaidya, V.K. (2015). Comparative study of biosorption of textile dyes using fungal biosorbents. Int. J. Curr. Microbiol. Appl. Sci., *4*(2): 357–365.

Sharma, K. and Parveen, S. (2011). Ecological study of fungi isolated from the surface water of Dudhawa Dam, Dhamtari, Chhattisgarh, India. J. Phytol., 3(4): 6–8.

Silva, F.; Nascimento, L. and Brito, M. (2019). Biosorption of methylene blue dye using natural biosorbents made from weeds. Mater. (Basel), 12(15): 2486. https://doi.org/10.3390/ma12152486

Smith, B. (2022). The infrared spectra of polymers, VI: Polymers with CO bonds. Spectroscopy, 15–19: 27. https://doi.org/10.56530/spectroscopy.ly3071f5

Srinivasan, N.; Thangavelu, K. and Sekar, A. (2021). *Aspergillus caespitosus* ASEF14, an oleaginous fungus as a potential candidate for biodiesel production using sago processing wastewater. Microb. Cell Fact., 20: 179. https://doi.org/10.1186/s12934-021-01667-3

Sylvia, N.; Dewi, R.; Fitriani, S. and Hakim, L. (2023). Adsorption of methylene blue on fixed bed column using adsorbent from tea waste. Int. J. Des. Nat. Ecodyn., 18(2): 251–259.

Szadkowski, B. and Marzec, A. (2024). Chitosan vs chitin: Comparative study of functional pH bioindicators synthesized from natural red dyes and biopolymers as potential packaging additives. Food Hydrocoll., 150:109670. https://doi.org/10.1016/j.foodhyd.2024.109670

Taha, A. and Gouda, S.A. (2025). Eco-friendly dye removal: Impact of dyes on aquatic and human health and sustainable fungal treatment approaches. Egypt. J. Aquat. Biol. Fish., 29(1): 2733–2763.

Taha, A.; Hussien, W. and Gouda, S.A. (2023b). Bioremediation of heavy metals in wastewaters: A concise review. Egypt. J. Aquat. Biol. Fish., 27(1): 143–166. https://doi.org/10.21608/ejabf.2023.284415

Taha, A.; Mohamed, S.; Mahmoud, M. A. *et al.* (2023a). Bioremoval of lead from polluted waters using the fungus *Talaromyces stipitatus* and its impact on male albino rats. Egypt. J. Aquat. Biol. Fish., 27(5): 429–462. https://doi.org/10.21608/ejabf.2023.319124

Tamura, K.; Stecher, G. and Kumar, S. (2021). MEGA11: Molecular evolutionary genetics analysis version 11. Mol. Biol. Evol. https://doi.org/10.1093/molbev/msab120

USEPA (United States Environmental Protection Agency). **(2002)**. Methods for measuring the acute toxicity of effluents and receiving waters to freshwater and

marine organisms (5th ed., EPA-821-R-02-012). U.S. Environmental Protection Agency.

Villegas-Navarro, A.; Rodriguez Santiago, M. and Ruiz Perez, F. (1997). Determination of LCs from *Daphnia magna* in treated industrial wastewaters and non-treated hospital effluents. Environ. Int., 23: 535–540.

Wang, F.; Li, L. and Iqbal, J. (2022). Preparation of magnetic chitosan corn straw biochar and its application in adsorption of amaranth dye in aqueous solution. Int. J. Biol. Macromol., 199: 234–242. https://doi.org/10.1016/j.ijbiomac.2021.12.195

Yang, Y.; Jim, D. and Wang, G. (2011). Biosorption of acid blue 25 by unmodified and CPC-modified biomass of *Penicillium* YW01: Kinetic study, equilibrium isotherm and FTIR analysis. Colloids Surf. B Biointerfaces, 88(1): 521–526. https://doi.org/10.1016/j.colsurfb.2011.07.047

Young, D.; Joshi, A. and Huang, L. (2022). Simultaneous metabarcoding and quantification of *Neocallimastigomycetes* from environmental samples: Insights into community composition and novel lineages. Microorganisms, 10: 1749. https://doi.org/10.3390/microorganisms10091749

Zango, Z.U.; Dennis, J.O.; Aljameel, A.I. (2022). Effective removal of methylene blue from simulated wastewater using ZnO–chitosan nanocomposites: Optimization, kinetics, and isotherm studies. Molecules, 27(15): 4746. https://doi.org/10.3390/molecules27154746

Zhang, F.; Song, W.J. and Lan, J. (2015). Effective removal of methyl blue by fine-structured strontium and barium phosphate nanorods. Appl. Surf. Sci., 326: 195–203. https://doi.org/10.1016/j.apsusc.2014.11.090